Available online at www.sciencedirect.com
SCIENCE DIRECT®
ELSEVIER
Earth and Planetary Science Letters 217 (2004) 245–261
EPSL
www.elsevier.com/locate/epsl

Lithium isotopic systematics of the mantle-derived ultramafic xenoliths: implications for EM1 origin

Yoshiro Nishio [a,b,*], Shun'ichi Nakai [b], Junji Yamamoto [c], Hirochika Sumino [c], Takuya Matsumoto [d], Vladimir S. Prikhod'ko [e], Shoji Arai [f]

[a] *Deep Sea Research Department, Japan Marine Science and Technology Center, 2-15 Natsushima, Yokosuka 237-0061, Japan*
[b] *Earthquake Research Institute, University of Tokyo, 1-1-1 Yayoi, Bunkyo-ku, Tokyo 113-0032, Japan*
[c] *Laboratory for Earthquake Chemistry, University of Tokyo, 7-3-1 Hongo, Bunkyo-ku, Tokyo 113-0033, Japan*
[d] *Department of Earth and Space Science, Osaka University, 1-1 Machikaneyama, Toyonaka, Osaka 560-0043, Japan*
[e] *Institute of Tectonics and Geophysics (Far-Eastern Branch, Russian Academy of Sciences), 65 Kim Yu Chen Street, Khabarovsk 680063, Russia*
[f] *Department of Earth Science, Kanazawa University, Kakuma, Kanazawa 920-1192, Japan*

Received 14 May 2003; received in revised form 2 September 2003; accepted 17 October 2003

Abstract

Isotopic signatures of mantle-derived xenoliths have provided much information on the evolution of their mantle source regions. A recently developed multiple-collector inductively coupled plasma mass spectrometry method allows precise and accurate lithium isotopic determinations of Li-poor samples such as peridotites. We present Li–Sr–Nd isotopic systematics of clinopyroxenes (CPXs) in mantle-derived ultramafic xenoliths. The results show that Ichinomegata (Northeastern Japan) and Bullenmerri (Southeastern Australia) samples have positive δ^7Li values (δ^7Li ~ +4 to +7‰, $\delta^7Li = [[^7Li/^6Li]_{sample}/[^7Li/^6Li]_{L-SVEC\ standard} - 1] \times 1000$) common to values previously reported for terrestrial volcanic rocks. By contrast, unusually low δ^7Li values (δ^7Li ~ −17‰) are observed in many samples from the Far East region of Russia (Sveyagin, Ennokentiev, and Fevralsky) and southwestern Japan (Kurose and Takashima). The δ^7Li values of Sikhote-Alin (Sveyagin and Ennokentiev) samples vary widely from −17.1‰ to −3.1‰, while the δ^7Li values are positively correlated with $^{143}Nd/^{144}Nd$, and negatively correlated with $^{87}Sr/^{86}Sr$. On the other hand, the δ^7Li values of the Bullenmerri samples are essentially constant (δ^7Li = +5.0 to +6.0‰), while the $^{87}Sr/^{86}Sr$ (0.7027 ~ 0.7098) and $^{143}Nd/^{144}Nd$ ratios (0.51224 ~ 0.51297) vary widely. These features can be explained by the results of a binary mixing between a depleted component (low-$^{87}Sr/^{86}Sr$, and high-$^{143}Nd/^{144}Nd$) and an enriched component (high-$^{87}Sr/^{86}Sr$, and low-$^{143}Nd/^{144}Nd$). The enriched component (metasomatic agent) in the mantle beneath the Sikhote-Alin area has extraordinarily low δ^7Li value (< −17‰), whereas the metasomatic agent in the mantle beneath the Bullenmerri area has positive δ^7Li value (+6‰). Based on the Sr–Nd isotopic systematics and coexistent hydrous mineral, metasomatic agents of the Sikhote-Alin and Bullenmerri samples are classified into anhydrous EM1-type and hydrous EM2-type, respectively. From these features, we infer that anhydrous EM1-like

* Corresponding author. Tel.: +81-468-67-9354; Fax: +81-468-67-9315.
E-mail addresses: nishio@jamstec.go.jp (Y. Nishio), snakai@eri.u-tokyo.ac.jp (S. Nakai), jyama@eqchem.s.u-tokyo.ac.jp (J. Yamamoto), sumino@eqchem.s.u-tokyo.ac.jp (H. Sumino), matsumoto@ess.sci.osaka-u.ac.jp (T. Matsumoto), vladimir@itig.as.khb.ru (V.S. Prikhod'ko), ultrasa@kenroku.ipc.kanazawa-u.ac.jp (S. Arai).

0012-821X/03/$ – see front matter
doi:10.1016/S0012-821X(03)00606-X

metasomatic agent may have an extremely low δ^7Li value, whereas hydrous EM2-like metasomatic agent may have a positive δ^7Li value. It has been predicted that the δ^7Li value of subducted highly altered mid-ocean ridge basalt (MORB) would be extremely low compared to that of fresh MORB due to the preferential loss of heavier Li (δ^7Li > altered MORB) from the subducted slab during dehydration at low temperature. Consequently, it is deduced that Li of metasomatic agent with an extremely low δ^7Li value is derived from subducted highly altered basalt. The enrichment of isotopically light Li (low δ^7Li) may be a general property of EM1 mantle reservoir. The Li isotopic data suggest further that the EM1 and HIMU sources originate from different parts of a recycling oceanic crust. This is essentially the same as the models proposed previously based on the radiogenic isotopic data, but with the Li isotopic data requiring uppermost, highly altered basaltic crust as well as pelagic sediment in the EM1 source, but not so in the HIMU end-member. Because of the apparent sensitivity of Li isotopic composition to the alteration profile of subducted MORB, it may provide complementary information to Sr, Nd, and Pb isotopic compositions regarding the mantle source.

Keywords: lithium isotope; mantle-derived xenolith; EM; HIMU; altered MORB; dehydration

1. Introduction

Understanding material cycles in the Earth's interior provides a better opportunity to study the evolution of the solid Earth. Lithium (Li) is a light alkali metal element. The large mass difference (~15%) between its two stable isotopes, ^{7}Li and ^{6}Li, produces large isotopic fractionation in terrestrial systems. Unlike radiogenic isotopic ratios, the Li isotopic ratio (^{7}Li/^{6}Li) is not affected by time or parent/daughter fractionation. Therefore, it is expected that Li isotopic compositions provide complementary information to familiar radiogenic isotopic compositions such as Sr, Nd, and Pb, regarding the geochemical reservoirs in the mantle.

Based on chondritic meteorite data, McDonough et al. [1] estimated a bulk solar system's δ^7Li value of ~ ±0‰ ($\delta^7\text{Li} = [[^7\text{Li}/^6\text{Li}]_{\text{sample}}/[^7\text{Li}/^6\text{Li}]_{\text{L-SVEC standard}} - 1] \times 1000$, $[^7\text{Li}/^6\text{Li}]_{\text{L-SVEC standard}} = 12.1163 + 0.0098$ [2]). The δ^7Li values of most terrestrial samples range between those of chondrite (ca. ±0‰ [1]) and those of seawater (ca. +30‰ [3–8]). Considering the Li budget of the terrestrial system, reservoirs having significantly low δ^7Li (< ±0‰) are likely to exist. Indeed, dramatically low δ^7Li values (−11 to +5‰) were recently reported for eclogites from Trescolmen, Switzerland [9]. Using an open-system Rayleigh distillation model, Zack et al. [9] demonstrated that the extremely low δ^7Li values of Trescolmen eclogites were the results of fluid loss (dehydration) of highly altered oceanic crust. The δ^7Li values of subducted altered mid-ocean ridge basalt (MORB) decrease after dehydration at a subduction zone [9], whereas those of altered MORBs (+4.5‰ to +14‰ [10,11]) are higher than those of fresh MORBs. The δ^7Li value of Li in dehydrated fluid is expected to be higher than that of residual slab Li [9]. By recycling such altered basalt, an isotopically light Li composition (δ^7Li < ±0‰) may be present in the solid earth [9], whereas δ^7Li values that are significantly lower than the chondritic values (ca. ±0‰) had never been observed in volcanic rock samples (+1.4 to +11.2‰) [2,7,10,12–19].

Mantle-derived ultramafic xenolith samples provide information about the mantle at a microscale, whereas volcanic rock samples integrate information about their source at a macroscale. Accordingly, it has been expected that δ^7Li heterogeneity in the mantle will be greater in xenoliths than lavas. Li isotopic data, however, are available for only one mantle-derived peridotite (a spinel lherzolite from the Red Sea) [15] since accurate and precise Li isotopic determinations of Li-poor samples such as peridotite have been difficult using conventional analytical methods by thermal ionization mass spectrometry (TIMS) [8,15]. This study uses a recently developed multiple-collector inductively coupled plasma mass spectrometry (MC-ICP-MS) method [8] that allows precise and accurate lithium isotopic determinations of Li-poor samples such as mantle peri-

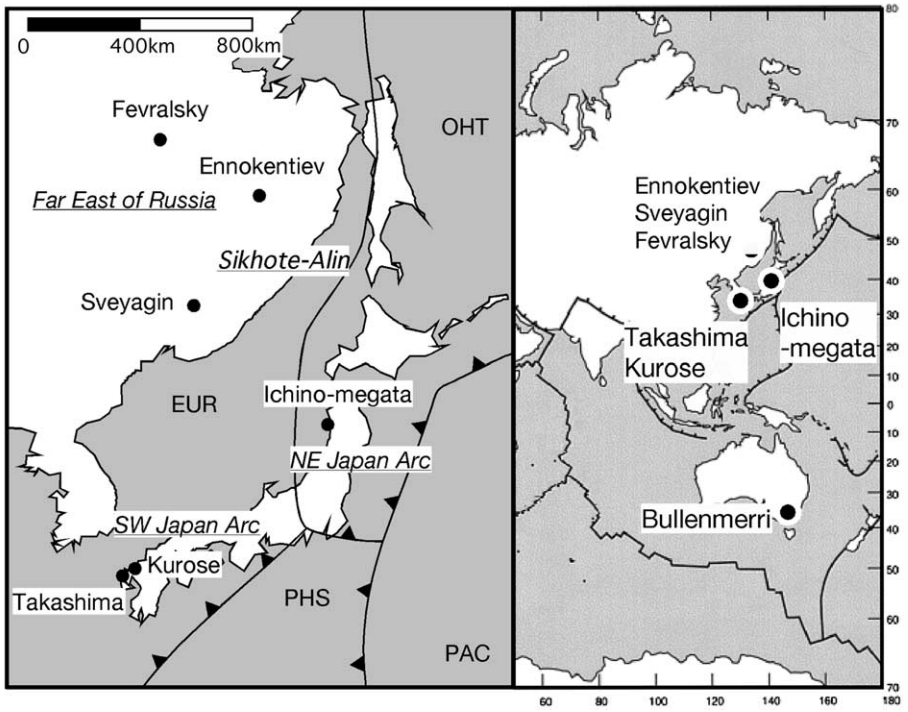

Fig. 1. Map showing locations for mantle-derived ultramafic xenolith samples studied. EUR, Eurasian plate; OHT, Okhotsk plate; PAC, Pacific plate; PHS, Philippine Sea plate.

dotites. We present a detailed data set of Li, Sr, and Nd isotopic compositions of clinopyroxenes (CPXs) from mantle-derived ultramafic xenoliths.

2. Sample descriptions and geological settings

We have analyzed CPXs separated from mantle-derived ultramafic xenoliths. The analyzed mantle-derived ultramafic xenoliths (lherzolite, harzburgite, dunite, clinopyroxenite, and CPX megacryst) from Cenozoic volcanic rocks come from Kurose and Takashima (Kyushu, southwestern Japan), Ichino-megata (Honshu, northeastern Japan), Bullenmerri (Newer Volcanics, Victoria, southeastern Australia), Sveyagin, Ennokentiev, and Fevralsky (the Far Eastern region, Russia). Of the Far Eastern Russian (hereafter FE Russian) sites, both Sveyagin and Ennokentiev are located on sites in the Sikhote-Alin ridge that stretches along the Pacific coast (Sea of Japan and Tatar Strait) from Vladivostok to the Amur River delta [20]. The sample localities are shown in Fig. 1.

Most of the analyzed xenoliths are spinel lherzolite, although the xenoliths from both Kurose and Takashima include harzburgite, dunite, clinopyroxenite, and CPX megacryst (Table 1). Arai et al. [21] classified the xenoliths from both Kurose and Takashima into three groups: mantle peridotite (lherzolite and harzburgite), dunite–wehrlite–pyroxenites of Group I, and pyroxenites of Group II. Dunite–wehrlite–pyroxenites of Group I have been considered to be cumulates, possibly produced from magma introduced into mantle peridotite, whereas pyroxenites of Group II have been considered to be cumulates from alkali basaltic melts genetically related to their host basalts [21]. Among the analyzed xenoliths, only the CPX megacryst (TKA0940) from Takashima belongs to Group II suites (Table 1). Spinel occurs in all the analyzed xenoliths, excluding one sample, the CPX megacryst (TKA0940) from Takashima.

Table 1
Li–Sr–Nd isotopic compositions of CPXs in mantle-derived xenoliths

Sample	Type[a]	δ^7Li[b] (‰)	$^{87}Sr/^{86}Sr$[b]	$^{143}Nd/^{144}Nd$[b]	Li[b] (ppm)	Sr[b] (ppm)	Nd[b] (ppm)	Separation date	Measurement date (δ^7Li)
Error (2σ)		±0.83	±0.00006	±0.000027	12%	10%	10%		
Ichino-megata (Honshu, Northeast Japan)									
IC97111401	Lh (n.d.)	+4.2	0.70310	b.d.	1.13	3.51	0.26	1/Mar./02	9/Mar./02
IC97111502	Lh (n.d.)	+6.8	0.70296	0.513213	1.25	6.82	2.71	18/Dec./01	16/Jan./02
Kurose (Kyushu, Southwest Japan)									
KRS9806	Du-GI (dry)	−7.7	0.70358	0.512882	24.0	18.7	1.27	12/Feb./02	9/Mar./02
KRS9814	Lh (dry)	−12.2	0.70333	b.d.	10.6	8.92	0.41	18/Feb./02	9/Mar./02
KU98101411	Hz (dry)	−11.9	0.70424	b.d.	13.5	8.20	0.25	18/Jan./02	2/Feb./02
Takashima (Kyushu, Southwest Japan)									
TKP1040	Pxn-GI (dry)	−9.8	0.70441	0.512769	2.22	22.1	1.28	12/Feb./02	9/Mar./02
TKA0940	Cpxm-GII (dry)	−6.6	0.70415	0.512743	3.20	51.7	9.61	18/Feb./02	9/Mar./02
TKD1350	Du-GI (dry)	−7.3	0.70465	0.512719	1.10	55.9	2.40	12/Feb./02	9/Mar./02
Sveyagin (Sikhote-Alin, the Far Eastern Region of Russia)									
Sv1-A[c]	Lh (dry)	−3.3	0.70242	0.513292	11.4	55.4	3.43	6/Jan./02	2/Feb./02
Sv1-B[c]	Lh (dry)	−3.1	0.70243	0.513273	11.2	51.6	3.31	6/Nov./02	2/Feb./02
Sv2F	Lh (dry)	−11.3	0.70300	0.513140	4.94	57.5	2.94	1/Mar./02	9/Mar./02
Ennokentiev (Sikhote-Alin, the Far Eastern Region of Russia)									
En1	Lh (dry)	−10.8	0.70367	0.512979	6.63	142	6.11	6/Jan./02	16/Jan./02
En2I-A[c]	Lh (dry)	−17.1	0.70359	0.512892	5.54	122	6.68	6/Jan./02	16/Jan./02
En2I-B[c]	Lh (dry)	−16.9	0.70364	0.512905	5.00	n.d.	n.d.	18/Feb./02	9/Mar./02
Fevralsky (the Far Eastern Region of Russia)									
Fev1	Lh (dry)	−4.0	0.70385	0.513119	7.54	60.8	4.31	6/Jan./02	16/Jan./02
Bullenmerri (Victoria, southeast Australia)									
9708	Lh (hyd)	+6.0	0.70982	0.512241	1.13	168	26.9	6/Mar./02	9/Mar./02
9894	Lh (dry)	+5.0	0.70275	0.512973	1.33	76.8	4.82	1/Mar./02	9/Mar./02
WGBM16	Lh (hyd)	+5.2	0.70395	0.512814	1.27	191	16.6	1/Mar./02	9/Mar./02
WGBM22	Lh (hyd)	+5.6	0.70479	0.512741	1.13	112	8.37	6/Mar./02	9/Mar./02

[a] Analyzed CPXs are from lherzolite (Lh), harzburgite (Hz), dunite (Du), clinopyroxenite (Pxn), and CPX megacryst (Cpxm). Most of the analyzed xenoliths are spinel lherzolite (mantle peridotite), although the xenoliths from both Kurose and Takashima contain harzburgite, dunite, clinopyroxenite, and CPX megacryst. Arai et al. [21] classified the xenoliths from both Kurose and Takashima into three types, which are: mantle peridotite (lherzolite and harzburgite), dunite–wehrlite–pyroxenites of Group I (GI) and pyroxenites of Group II (GII) (see text for sample descriptions). Xenoliths are divided into two types. One is the anhydrous (dry) type that is free of amphibole, the other is hydrous (hyd) type that contains amphibole.

[b] $\delta^7Li\ (‰) = ([^7Li/^6Li]_{sample}/[^7Li/^6Li]_{L-SVEC\ standard} - 1) \times 1000$. The $^{87}Sr/^{86}Sr$ and $^{143}Nd/^{144}Nd$ data were normalized to: $^{87}Sr/^{86}Sr = 0.710258$ for SRM987, and $^{143}Nd/^{144}Nd = 0.5121067$ for JNdi-1. Measurements below the detection limit are listed as 'b.d.'. No data are listed as 'n.d.'.

[c] Only samples Sv1 and En2I were analyzed twice (A and B, respectively). Two analyses, A and B, were prepared from different aliquots in a xenolith. All samples (excluding Sv1-A) were washed in 5% HNO_3. Only Sv1-A was washed in 33% HNO_3.

The analyzed xenoliths from Sveyagin, Ennokentiev, Fevralsky (FE Russia), Kurose, and Takashima (SW Japan) are amphibole-free, whereas several Bullenmerri (SE Australia) xenoliths contain amphibole. Modal compositions for the Ichino-megata (NE Japan) xenoliths were not determined owing to their small size, although previous work indicated that more than half of the Ichino-megata xenoliths were hydrous, containing pargasitic amphibole [22,23]. These amphiboles have been considered to be mantle metasomatic minerals, caused by the addition of hydrous melt/fluid to dry peridotite [24–26]. Previous studies also indicated that hydrous minerals such as amphibole were not detected in the xenoliths from Sikhote-Alin (FE Russia) [20], Kurose [21,23], and Takashima [21].

The host lavas of Takashima and Kurose sam-

ples erupted 3 Ma [27] and 1 Ma [28], respectively. The host lavas of Ichino-megata and Bullenmerri samples erupted ca. 9000 yr ago [29] and ca. 20,000–25,000 yr ago [30], respectively. In the Sikhote-Alin region, xenolith-bearing volcanism commenced at 20 Ma [20,31]. It is widely accepted that the Quaternary volcanism of NE Japan is due to the subduction and dehydration of the Pacific plate [32,33]. By contrast, it has been proposed that Cenozoic alkalic volcanism in SW Japan may have been caused by a mantle plume [34–37]. According to geodynamic reconstructions [38], the Sikhote-Alin (FE Russia) region was an active margin of the Asian continent in Mesozoic to Paleogene times. Indeed, lavas with typical arc magma chemistry were produced at 40–25 Ma in the eastern part of the Sikhote-Alin region [31]. After a volcanic hiatus at 25–20 Ma, intraplate-type lavas with typical hotspot magma compositions have dominated magmatism in both the eastern and western Sikhote-Alin region since 20 Ma [31]. Several authors have suggested that such intraplate magmatism may be caused by mantle plumes [39–42].

Some Takashima xenoliths (dunite) show significantly high $^3He/^4He$ ratios ($\sim 17.9R/R_A$) compared to the MORB value ($8R/R_A$) (the $^3He/^4He$ ratios are expressed relative to the atmospheric ratio, $R_A = 1.4 \times 10^{-6}$) [43]. This means that some Takashima xenoliths contain primordial helium that should reside in the lower mantle. In addition, the apatite in spinel lherzolites from Bullenmerri (SE Australia) has a neon-isotope signature similar to that associated with plume-related volcanism, as is found in Hawaii [44]. Detailed petrological descriptions for the samples studied here are given by Griffin et al. [45] for Bullenmerri; Takahashi [46] and Abe et al. [23,47] for Ichino-megata; and Arai et al. [21] for Kurose and Takashima.

3. Analytical method

Nishio and Nakai [8] reported an accurate and precise Li isotope analytical method using MC-ICP-MS. In this study, Sr and Nd isotope ratios and concentrations have been measured together with Li isotopic composition. Because of this, we have modified the method of Nishio and Nakai [8] as follows.

3.1. Sample preparation

After repeated crushing of the mantle-derived ultramafic xenoliths, fresh CPXs were handpicked under a binocular microscope to avoid contamination. Collected CPXs were washed ultrasonically in a 5% HNO_3 solution (15 min) and then cleaned ultrasonically in Milli-Q water (15 min), twice. As there is a possibility that a strong acid leaching may cause Li isotopic fractionation, samples were washed with a dilute acid (5% HNO_3). Sample Sv1-A was washed with 33% HNO_3 (15 min) to investigate acid leaching effects. After drying at 110°C for 24 h, the CPXs were crushed to powder using an agate mortar. Powdered samples (50 mg) were weighed into screw-cap Savillex beakers. Concentrated HF (49%, 0.6 ml) and $HClO_4$ (60%, 0.3 ml) were used for digestion of the CPX samples. This digested solution was evaporated. Prior to complete evaporation, several drops of concentrated $HClO_4$ were repeatedly added to remove any organic materials derived from the samples. The dried residues were redissolved in 33% HNO_3 (3 ml) at 150°C for 12 h. The completely decomposed sample was then evaporated, and the residue was dissolved in 10 ml of 9.3% HNO_3 (with trace HF), and a portion of this dissolved solution was used for the measurements of Sr and Nd contents. The remainder was evaporated and dissolved in 4.7% HNO_3 (6 ml). Prior to column separation, 3 ml of methanol was added. Therefore, the sample solution for column loading was 9 ml of 3% HNO_3 in 33% methanol.

3.2. Column separation

Cation exchange resin, Bio-Rad AG 50W-X8 (200–400 mesh), was packed into columns (quartz glass, with an internal diameter of 6 mm), to a height of 125 mm. The resin was cleaned by repeated rinses with 20% HCl, 33% HNO_3, and Milli-Q water, sequentially. Before sample loading, the resin was conditioned with 15 ml of

Table 2
The Li isotopic ratios on our in-house Li standard solution (+15.08 ± 0.82 ‰, 2σ) [8]

Measurement date	δ^7Li (‰)
16/Jan./02	+14.40
2/Feb./02	+14.83
9/Mar./02	+15.53

0.47% HNO_3 in 50% methanol. After sample loading, 128 ml of 4.7% HNO_3 in 80% methanol was passed; the first 13 ml were discarded, and the following 115 ml were collected for Li at a rate of 0.16 ml/min.

After Li extraction, 85 ml of 6.6% HCl was passed, the first 65 ml of which were discarded and the following 20 ml were collected for Sr (+Ca). Then 20 ml of 20% HCl was passed, the first 10 ml of which were discarded and the following 10 ml were collected for light rare earth elements (LREEs) including Nd. Because of abundant Ca in CPX, Sr was additionally purified using Sr-resin (Eichrom). Separation of Nd from other LREEs was performed using Ln-resin (Eichrom). Procedural blanks for Li, Sr, and Nd isotopic analyses were less than 10, 50, and 10 pg, respectively.

3.3. Mass spectrometry

Li, Sr, and Nd isotopic ratios were measured in solutions containing about 100 ppb Li, 100 ppb Sr, and 50 ppb Nd, respectively, using MC-ICP-MS (Isoprobe, Micromass). Samples were introduced into the spectrometer via a Cetac Aridus desolvating unit. For Sr and Nd isotopic measurements, the existing (normal) Cetac nebulizer (T1H) was replaced with a micromist nebulizer from Glass Expansion Pty. Ltd. Li abundances were also measured using the MC-ICP-MS. For Li isotopic analyses, samples were bracketed by a Li standard solution (NIST L-SVEC) to correct the isotopic compositions for instrumental mass bias. Measured Li isotopic ratios are expressed as $\delta^7\mathrm{Li} = ([^7\mathrm{Li}/^6\mathrm{Li}]_{\mathrm{sample}}/[^7\mathrm{Li}/^6\mathrm{Li}]_{\mathrm{L-SVEC\ standard}} - 1) \times 1000$. In this study, Li isotopic measurements by MC-ICP-MS were performed on three separate days (16/Jan./02, 2/Feb./02, and 9/Mar./02). The δ^7Li data for our in-house Li standard solution [8] for these days are listed in Table 2. The results (+14.4 to +15.5 ‰) are in accordance with the long-term (23/Oct./00 to 26/Jan./01) average value of +15.1 ‰ within analytical error (± 0.8 ‰, 2σ) (Table 2). Following the Li isotopic measurement, we monitored the solutions for coexisting ions, such as C, Na, Mg, Al, Ca, and Fe, to ensure that their abundances were too low to cause any matrix effect. The Li concentrations were estimated from the comparison of beam intensities of $^7Li^+$ in the sample solution with that of a standard solution. In this case, analytical error for Li concentrations is better than 12% at 2σ, as esti-

Table 3
Comparison of our $^{87}Sr/^{86}Sr$ and $^{143}Nd/^{144}Nd$ ratios of reference rock samples (JA-1) with previously reported values

$^{87}Sr/^{86}Sr$ ± 2σ	$^{143}Nd/^{144}Nd$ ± 2σ	Reference
0.70360 ± 0.00006	**0.513083 ± 0.000006**	**This study**
(*n* = 6)	**(*n* = 3)**	
0.703557 ± 0.000018	0.513078 ± 0.000008	Orihashi et al. (1998) [57]
0.703533 ± 0.000010	0.513066 ± 0.000010	Na et al. (1995) [56]
0.703572 ± 0.000008		Iizumi et al. (1994) [55]
	0.513086 ± 0.000005	Arakawa (1992) [54]
0.703637 ± 0.000012		Notsu and Hirao (1990) [53]
0.70363 ± 0.00001	0.5130880.000008	Okano et al. (1989) [52]
0.703507 ± 0.000016	0.513065 ± 0.000010	Kagami et al. (1989) [51]
0.70367 ± 0.00005		Zhang Zichao (1987)[a] [50]
0.703636 ± 0.000010		Shirahase and Nakajima (1984)[a] [50]
0.703586 ± 0.000011		Kurasawa (1984) [49]

Bold type: mean and standard deviation on separate measurements.
[a] Personal communication in Ando and Shibata [50].

mated from the reproducibility of standard rocks [8]. Detailed Li analytical procedures, including accuracy and precision, have been previously documented [8]. The $^{87}Sr/^{86}Sr$ and $^{143}Nd/^{144}Nd$ data were normalized to $^{87}Sr/^{86}Sr = 0.710258$ for SRM987, and to $^{143}Nd/^{144}Nd = 0.5121067$ for JNdi-1. A high-grade argon (Ar) carrier gas was used for the Sr isotopic measurement, compared to Li–Nd isotopic measurement, as low-grade Ar gas contains noble gases such as krypton (Kr), which interfere with accurate and precise Sr isotopic measurements. Before Sr isotopic measurements, we checked that peaks around *m/e* 83 (Kr) were under the detection limit ($< 10^{-15}$ A). The $^{87}Sr/^{86}Sr$ and $^{143}Nd/^{144}Nd$ data for the reference rock sample (JA-1, andesite [48]) are listed in Table 3, together with other published data [49–57]. Our $^{87}Sr/^{86}Sr$ and $^{143}Nd/^{144}Nd$ data for the standard rocks agree well with previously published data.

The concentrations of Sr and Nd were determined using a quadrapole ICP-MS (PQ3, Thermo Elemental) without purification using a method in which the matrix effect was corrected by internal standards of indium (In) and rhenium (Re). In this case, both analytical errors for Sr and Nd concentrations are better than 10% (2σ), as estimated from the reproducibilities of standard rocks.

4. Results

The abundances and isotopic ratios of Li of CPXs from the mantle-derived xenoliths are listed in Table 1, together with those of Sr and Nd. Li isotopic ratios of the CPXs vary widely ($\delta^7Li = -17.1$ to $+6.8$ ‰) (Table 1). Among the analyzed mantle-derived xenoliths, Ichino-megata (NE Japan, $\delta^7Li = +4.2$ to $+6.8$ ‰) and Bullenmerri (SE Australia, $\delta^7Li = +5.0$ to $+6.0$ ‰) samples have positive δ^7Li values (Table 1), which are similar to those of volcanic rocks from convergent plate margins [2,13–16]. In contrast, low δ^7Li values were observed in mantle-derived xenoliths from Kurose (~ -12.2 ‰), Takashima (~ -9.8 ‰), Sveyagin (~ -11.3 ‰), Ennokentiev (~ -17.1 ‰), and Fevralsky (-4.0 ‰) (Table 1). These δ^7Li values are extremely low in comparison with previously reported δ^7Li values of volcanic rock samples (+1.4 to +11.2 ‰) [2,7,10,12–19] and with the Ichino-megata and Bullenmerri samples reported here. En2I from Sikhote-Alin (FE Russia), the lowest δ^7Li sample, was analyzed twice using different aliquots from the same xenolith. The measured δ^7Li values of En2I-A (-17.1 ‰) and En2I-B (-16.9 ‰) agree within analytical error (± 0.8 ‰, 2σ). As mentioned in Section 2, most of the analyzed xenoliths are spinel lherzolite, although the xenoliths from both Kurose and Takashima include harzburgite, dunite, clinopyroxenite, and CPX megacryst (Table 1). Both Kurose and Takashima were classified into three groups: mantle peridotite (lherzolite and harzburgite), dunite–wehrlite–pyroxenites of Group I, and pyroxenites of Group II [21]. The samples from Kurose and Takashima, regardless of classification, contain lithium with negative δ^7Li value. The CPXs of FE Russia (5–11 ppm Li) and Kurose (11–24 ppm Li) xenoliths contain abundant Li, compared to the Ichino-megata (1 ppm), Bullenmerri (1 ppm), and Takashima (1–3 ppm) xenoliths.

The results show that Sr and Nd isotopic ratios of CPXs from mantle-derived ultramafic xenoliths vary widely ($^{87}Sr/^{86}Sr = 0.7024$–0.7098 and $^{143}Nd/^{144}Nd = 0.51224$–$0.51329$) (Table 1). The $^{87}Sr/^{86}Sr$ and $^{143}Nd/^{144}Nd$ ratios of the analyzed FE Russian samples (Sveyagin, Ennokentiev, and Fevralsky) range from 0.7024 to 0.7037 and from 0.51289 to 0.51329, respectively (Table 1). Among the samples from the three regions, the Ennokentiev and Fevralsky samples contain more radiogenic Sr and less radiogenic Nd ($^{87}Sr/^{86}Sr = 0.7036$–0.7039 and $^{143}Nd/^{144}Nd = 0.51289$–$0.51312$) compared with those from Sveyagin ($^{87}Sr/^{86}Sr = 0.7024$–0.7030 and $^{143}Nd/^{144}Nd = 0.51314$–$0.51329$) (Table 1). Sv1, one of the Sveyagin samples, has the lowest $^{87}Sr/^{86}Sr$ (0.7024) and highest $^{143}Nd/^{144}Nd$ (0.51327–0.51329) among the analyzed samples. Analyzed Ichino-megata samples have also low $^{87}Sr/^{86}Sr$ (0.7030–0.7031) and high $^{143}Nd/^{144}Nd$ (0.51321) ratios, which range within the previously reported Ichino-megata values (CPX data from lherzolites, harzburgite, and websterite: $^{87}Sr/^{86}Sr = 0.7027$–

0.7046 and $^{143}Nd/^{144}Nd = 0.51283–0.51336$) [58]. The Sr and Nd isotopic ratios found in samples from Kurose ($^{87}Sr/^{86}Sr = 0.7033–0.7042$ and $^{143}Nd/^{144}Nd = 0.51288$) and Takashima ($^{87}Sr/^{86}Sr = 0.7042–0.7047$ and $^{143}Nd/^{144}Nd = 0.51272–0.51277$) are more radiogenic than those found in analyzed Ichino-megata samples. The $^{87}Sr/^{86}Sr$ and $^{143}Nd/^{144}Nd$ ratios of the analyzed Bullenmerri samples vary widely, from 0.7027 to 0.7098 and from 0.51224 to 0.51297, respectively.

5. Discussion

5.1. The accuracy of extremely low δ^7Li values

Extremely low δ^7Li values ($\delta^7Li \sim -17‰$) were measured in CPXs from several mantle-derived ultramafic xenoliths using MC-ICP-MS. Compared to TIMS, the MC-ICP-MS technique enables high-precision analyses ($\pm 0.82‰$, 2σ) with small amounts of Li ($\sim$45 ng Li) [8]. Consequently, only 50 mg of rock sample is sufficient to determine the accurate Li isotopic composition of a low Li-concentration sample (1 ppm Li at least). A small amount of ions introduced into the column chromatography inhibits any shift in the Li elution peak during column separation. In addition, the smaller matrix effect of the MC-ICP-MS technique allows the collection of a larger fraction in the column chromatography to avoid Li loss. We collected a large volume of effluent (13–128 ml) for the Li fraction, whereas most Li is eluted from 50 to 100 ml [8].

The low Si contents (equivalent to high Mg in the case of mantle-derived samples) of analyzed samples are one cause of the measured δ^7Li value being lower than the true value (details are described in the Appendix). However, the Si (Mg) contents of the CPXs with extremely low δ^7Li values are approximately equal to those CPXs with positive δ^7Li values (Table 4) [45,59]. Furthermore, several samples with extremely low δ^7Li (FE Russia and Kurose) are enriched in Li relative to basalts (ca. 5 ppm Li) (Table 1). Because the Li concentration of the solution introduced into the MC-ICP-MS is fixed at 100 ppb Li in our analytical protocol, concentrations of coexistent ions tend to decrease with increasing Li contents in the analyzed samples. In addition, both extremely low and positive δ^7Li data were measured on the same day (see Table 1). Because instrumental conditions (i.e. location of detector and focusing) have not been changed during sequential measurements conducted on the same day, the extremely low δ^7Li values observed in this study are not due to the instrumental condition of the MC-ICP-MS.

Table 4
Comparison of major elemental compositions of CPXs with extremely low and positive δ^7Li values

	Sikhote-Alin		Bullenmerri[a]	
	En2	Sv1	dry	hyd
δ^7Li (‰)[b]	−17	−3	+5	+5 to +6
SiO_2 (wt%)	52	53	52–54	53–54
TiO_2 (wt%)	0.5	0.6	0.1–0.4	0.0
Al_2O_3 (wt%)	6.8	7.2	3.8–5.0	3.9–4.5
Cr_2O_3 (wt%)	0.7	0.5	0.7–1.3	1.2–1.4
FeO^T (wt%)	3.2	2.7	2.3–3.9	2.2–3.1
MnO (wt%)	0.1	0.1	0.0–0.1	0.1
MgO (wt%)	15	15	15–16	15
NiO (wt%)	0.0	0.0	0.0	0.0–0.1
CaO (wt%)	20	20	20–22	21
Na_2O (wt%)	1.9	1.7	1.3–1.7	1.8–1.9
References[c]	[59]	[59]	[45]	[45]

[a] Mantle-derived xenoliths in Bullenmerri are divided into two types. One is the anhydrous (dry) type that is free of amphibole, the other is the hydrous (hyd) type that contains amphibole.
[b] δ^7Li values are the results of this study.
[c] References of major element data.

5.2. The features of extremely low δ^7Li component in mantle-derived xenoliths

5.2.1. Anhydrous metasomatic agent

Correlations are observed in the Sikhote-Alin (Sveyagin and Ennokentiev) data; the δ^7Li is positively correlated with $^{143}Nd/^{144}Nd$ (Fig. 2a), and negatively correlated with $^{87}Sr/^{86}Sr$ (Fig. 2b). The wide δ^7Li variation of the Sikhote-Alin samples can be explained as a result of mixing between a depleted component (high-δ^7Li, low-$^{87}Sr/^{86}Sr$, and high-$^{143}Nd/^{144}Nd$) and an enriched component (low-δ^7Li, high-$^{87}Sr/^{86}Sr$, and low-$^{143}Nd/^{144}Nd$). This indicates that the enriched component (the metasomatic agent) in the mantle beneath the Si-

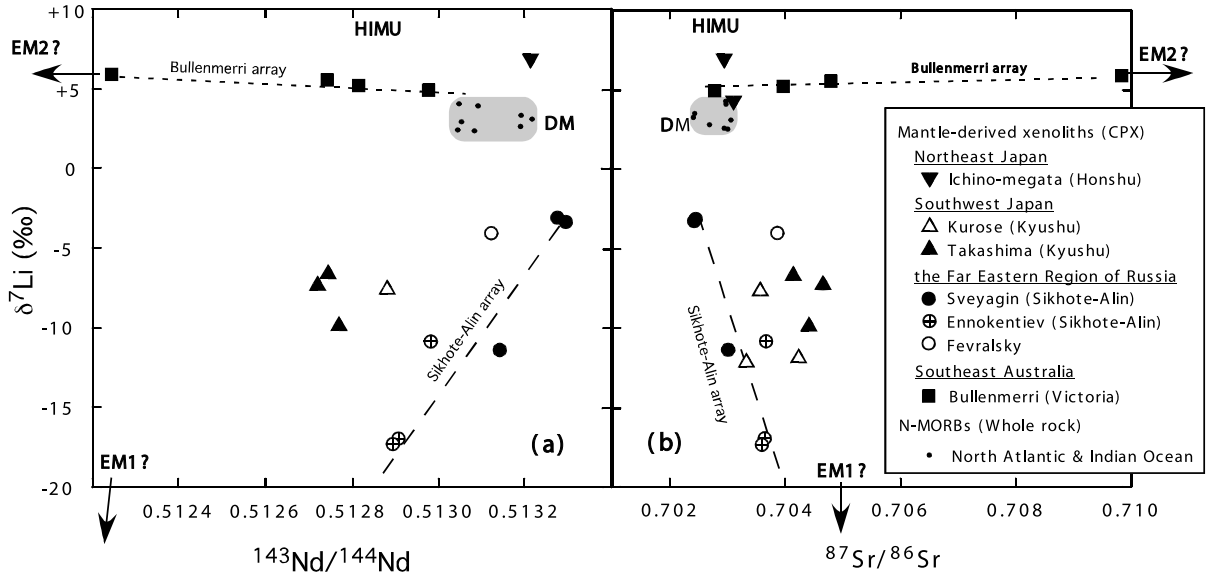

Fig. 2. δ^7Li values as a function of the ^{143}Nd/^{144}Nd (a) and ^{87}Sr/^{86}Sr ratios (b) of CPXs in the mantle-derived ultramafic xenoliths. Both diagrams show the positions of the mantle reservoirs identified by Zindler and Hart [61], Nishio et al. [16,18,19], and this study: DM, depleted mantle; EM1 and EM2, enriched mantle; HIMU, mantle with high U/Pb ratio. The short-dashed and long-dashed lines are best-fit regression lines of the Bullenmerri and Sikhote-Alin samples, respectively. Correlations are observed in the Sikhote-Alin (Sveyagin and Ennokentiev) data; the δ^7Li is positively correlated with ^{143}Nd/^{144}Nd (panel a), and negatively correlated with ^{87}Sr/^{86}Sr (panel b). In contrast to this, the δ^7Li values of the Bullenmerri samples are essentially constant, whereas their ^{87}Sr/^{86}Sr and ^{143}Nd/^{144}Nd ratios vary widely (panels a and b). The distributions of N-MORB data (MORBs which have chondrite-normalized La/Sm ratios are less than 1) are hatched. The N-MORB data are from Nishio's unpublished data (δ^7Li = +3.2 ± 1.4‰, 2σ [16]).

khote-Alin area has an extraordinarily low δ^7Li value (lower than −17‰).

In contrast, the δ^7Li values of the Bullenmerri samples are essentially constant (δ^7Li = +5.0 to +6.0‰), whereas their ^{87}Sr/^{86}Sr (0.7027–0.7098) and ^{143}Nd/^{144}Nd ratios (0.51224–0.51297) vary widely (Fig. 2a,b). These wide Sr and Nd isotopic variations have been considered to result from binary mixing, as Sr and Nd isotopic ratios are also correlated with carbon isotopic ratios (δ^{13}C) [58]. No obvious correlation between ^{87}Sr/^{86}Sr and ^{87}Rb/^{86}Sr ratios supports the binary mixing model, too [60]. The Bullenmerri anhydrous lherzolites have a relatively limited range of ^{87}Sr/^{86}Sr and ^{143}Nd/^{144}Nd ratios, whereas the ratios found in hydrous xenoliths are more radiogenic [60], which is also shown in the results of this study (Table 1). From these viewpoints, it has been considered that the metasomatic agent with the enriched signature (high-^{87}Sr/^{86}Sr and low-^{143}Nd/^{144}Nd) observed in the Bullenmerri samples is hydrous [60]. It is notable that the metasomatic agent observed in Ichino-megata samples is also hydrous [22,23]. Although there are only two data, the δ^7Li values of the Ichino-megata xenoliths are positive (+4.2 to +6.8‰), similar to the Bullenmerri samples. By contrast, the Sikhote-Alin (Sveyagin and Ennokentiev), Kurose, and Takashima xenoliths with extremely low δ^7Li values are free of hydrous minerals (Table 1). From these observations, we infer that anhydrous metasomatic agents may be characterized by extremely low δ^7Li values.

5.2.2. *EM1-like metasomatic agent*

At least four end-member components have been proposed: depleted mantle (DM), high U/Pb mantle (HIMU), and enriched mantle (EM1 and EM2) (e.g. [61]) to explain the Sr, Nd, and Pb isotopic systematics of ocean island basalts (OIBs). Zindler and Hart [61] noticed that mantle-derived xenoliths appeared to show similar iso-

topic variations and they classified metasomatic agents, which have caused the isotopic variations, into two types based on Sr–Nd isotopic systematics of the xenoliths. One has an EM1-like signature; the other has an EM2-like signature. In addition, they suggested that EM1-like metasomatic agent is anhydrous (CO_2-rich fluids), whereas EM2-like metasomatic agent is hydrous [61,62]. It is unknown whether the processes that formed these types of metasomatic agents were the same as those that formed OIB end-members, but the apparent similarity in their isotopic systems may imply a genetic relationship [61].

The Sr–Nd isotopic diagram (Fig. 3) shows that the trend of the Sikhote-Alin (Sveyagin and Ennokentiev) array differs from that of the Bullenmerri array. In this figure both arrays show a decrease of $^{143}Nd/^{144}Nd$ ratios when the $^{87}Sr/^{86}Sr$ ratios increase. However, the Sikhote-Alin array shows a faster decrease than the Bullenmerri array and the extension of both arrays leads to EM1 and EM2 end-members, respectively. From these features, we infer that classification of enriched components (metasomatic agents) on the basis of Li isotopic composition (extremely low δ^7Li versus positive δ^7Li) may correspond with the Sr–Nd isotopic systematics of the mantle-derived xenoliths.

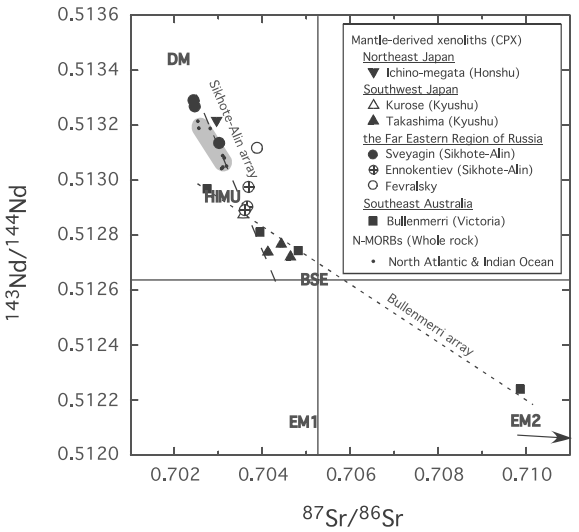

Fig. 3. The correlation diagram of Sr–Nd isotopic ratios of CPXs in the mantle-derived ultramafic xenoliths. This diagram shows the positions of the mantle reservoirs identified by Zindler and Hart [61]: BSE, bulk silicate Earth. Other symbols are the same as in Fig. 2. The trend of the Sikhote-Alin (Sveyagin and Ennokentiev) array differs from that of the Bullenmerri array. Both arrays show a decrease of $^{143}Nd/^{144}Nd$ ratios when the $^{87}Sr/^{86}Sr$ ratios increase. However, the Sikhote-Alin array shows a faster decrease than the Bullenmerri array and the extension of both arrays leads to EM1 and EM2 end-members, respectively. The distribution of N-MORB data (MORBs which have chondrite-normalized La/Sm ratios are less than 1) is hatched. The N-MORB data are from Nishio's unpublished data.

The enriched component (metasomatic agent) of the Bullenmerri xenoliths seems to have an EM2-like isotopic signature judging from the extension of the trend in Fig. 3. Previously reported Pb isotopic data also support the metasomatic agent of Bullenmerri having the EM2-like signature [58]. On the basis of our Bullenmerri data, then, the δ^7Li value of the EM2-like end-member component (metasomatic agent) is estimated to be +6‰, which is slightly higher than that of DM. The δ^7Li value of the DM component is estimated as $+3.2 \pm 1.4$‰ (2σ, $n = 8$) from the results of fresh N-MORB glasses (chondrite-normalized La/Sm ratios are less than 1) that were recovered from the Mid-Atlantic and the Indian Ocean [16].

In contrast, the Sr–Nd isotopic array of the Sikhote-Alin region (Sveyagin and Ennokentiev) is significantly different (Fig. 3): As the extension of $^{87}Sr/^{86}Sr$–$^{143}Nd/^{144}Nd$ correlation for Sikhote-Alin samples leads to the EM1 end-member, it is inferred that the metasomatic agent with extremely low δ^7Li value has an EM1-like signature (Fig. 3). From the Pb–Sr–Nd isotopic systematics, it has been pointed out that the volcanic rocks and mantle-derived ultramafic xenoliths from the eastern margin of the Eurasian plate (including the FE Russia and SW Japan regions) show EM1-like signatures [41,63–68]. The SW Japan samples (Kurose and Takashima) analyzed in this study have extremely low δ^7Li values as well as FE Russian samples. The features described above, therefore, support the possibility that the extremely low δ^7Li may be characteristic of EM1-like metasomatic agent. Furthermore, as described previously, it has been suggested that EM1-like metasomatic agent is anhydrous (CO_2-rich fluids), whereas EM2-like metasomatic agent is hydrous [61,62]. Our observation that xenoliths

from Sikhote-Alin (Sveyagin and Ennokentiev), Kurose, and Takashima with extremely low δ^7Li values are free of hydrous minerals seems to be consistent with our model.

5.3. Origin of Li of metasomatic agent with extremely low δ^7Li

Li isotopic fractionation at magmatic temperatures is small [12]. As stable isotope fractionation factors are temperature-dependent, it is expected that large Li isotopic fractionation would occur with Li differentiation at low temperature. Recently, Zack et al. [9] proposed that subducted highly altered oceanic crust should be characterized by significantly low δ^7Li values ($<$ fresh MORB), due to preferential loss of heavier Li (higher δ^7Li) from the subducting slab during dehydration at low temperatures (close to the trench). This model was derived from a finding of dramatically low δ^7Li values (-11‰ to +5‰) in eclogites from Trescolmen, Switzerland [9]. Before the study of Zack et al. [9], δ^7Li values that are significantly lower than the chondritic values (ca. $\pm$0‰ [1]) had never been observed in terrestrial samples (e.g. [2–8,10–17,69–71]). The Trescolmen eclogites have been considered to be an analog for subducted oceanic crust [9,72]. Using an open-system Rayleigh distillation model, Zack et al. [9] demonstrated that the extremely low δ^7Li values of several Trescolmen eclogites were the results of fluid loss (dehydration) of highly altered oceanic crust.

The δ^7Li values of subducted altered MORB decrease after dehydration at a subduction zone [9], whereas those of altered MORBs (+4.5 to +14‰ [10,11]) are higher than that of fresh MORB (+1.5 to +6.8‰ [2,10,16]). The δ^7Li value of Li in dehydrated fluid is expected be higher than that of residual slab Li [9]. Indeed, fluids from the decollement of the Costa Rica subduction zone [71] and fluids associated with the Conical serpentine seamount [73] support this model. In both cases, the subduction fluids have δ^7Li of about +20‰, significantly higher than that of altered MORB and hemipelagic sediments from which they are derived (δ^7Li $<$ +14‰) [11,71].

Here, in the Li isotopic fractionation model of Zack et al. [9], the most important point is that the more a basalt has been altered, and has high δ^7Li, the lower δ^7Li the rock will have after dehydration [9]. During low-temperature alteration at the seafloor, both Li concentrations and δ^7Li values increase with the degree of alteration [9]. In addition, the abundance of H_2O bound on the interlayer sites of clays increases with the degree of alteration [9]. Due to the large potential volume of water for dehydration, the δ^7Li value of highly altered basalt becomes lower following dehydration, compared to slightly altered basalt [9]. For example, it was calculated that highly altered basalt with 8 wt% interlayer-bound H_2O, 80 ppm Li and δ^7Li of +14‰, becomes δ^7Li of -10‰ and 20 ppm Li [9]. By contrast, it was calculated that slightly altered basalt with 1 wt% interlayer-bound H_2O, 15 ppm Li and δ^7Li of +5.5‰, becomes δ^7Li of +3‰ and 10 ppm Li [9]. Consequently, it is deduced that Li of metasomatic agent with an extremely low δ^7Li value is derived from subducted highly altered basalt. It is also notable that both highly and slightly altered MORBs still retain higher Li abundance even after dehydration, in comparison with mantle peridotite [9] and that the addition of a minute amount of metasomatic agent would cause a large decrease in δ^7Li of the metasomatized xenoliths.

5.4. Implication for EM1 origin

As discussed in Section 5.2.2, we infer that the extremely low δ^7Li value may be a property of the EM1-like metasomatic agent. As a lack of ‰-level Li isotopic fractionation at magmatic temperature [12], the Li isotopic composition of the metasomatic agent generated at high temperature would be approximately equal to that of the parent source (ex. dehydrated slab residue Li). However, it has not been revealed whether the root slab resided at shallow levels in the convecting mantle (ex. sub-continental mantle) or was cycled through the deep mantle.

Recently, Kobayashi et al. [74] reported the extremely low δ^7Li values (>-10.2‰) of glass inclusions from fresh picritic lavas from the Oahu North-a (Hawaii). In addition, the δ^7Li values of several Koolau lavas (2–3‰) are slightly lower

than those of fresh N-MORBs [17]. Low $^{206}Pb/^{204}Pb$ ratios between about 17.5 and 18.0 are characteristic of EM1-enriched oceanic island and seamount volcanoes such as Oahu North-a and Koolau lavas [75,76]. Therefore, we infer that isotopically light Li enrichment ($\delta^7Li <$ fresh MORB) may be a general property of EM1 mantle reservoir. As well as EM1-like metasomatic agent, most Li of the EM1 reservoir may originate from Li of highly altered basalt, as represented by the uppermost part of the oceanic crust.

Based on the distribution of Sr–Nd–Pb isotopic data of OIBs, it was proposed that the HIMU reservoir is closely related to the EM1 reservoir (e.g. [77]). Moreover, several authors proposed that the EM sources were derived from the ancient dehydrated subducted basalt (the HIMU source) contaminated with small amounts of sedimentary components (e.g. [78–80]). Although the basaltic portion evolved with high $^{238}U/^{204}Pb$ ($\mu \sim 22$) and low $^{232}Th/^{238}U$ ($\kappa \sim 3.2$), the high U, Th, and Pb of sediments dominate the isotopic evolution of the basaltic crust and sediment mixture [79]. A mixture of old basaltic crust and pelagic sediment ($\mu \sim 5$ and $\kappa \sim 6$) may produce EM1, while a mixture of old basaltic crust and terrigenous sediment ($\mu \sim 10$ and $\kappa \sim 4.5$) may produce EM2 [79]. As well as Pb isotopic compositions, this model [79] can explain the Sr–Nd isotopic compositions of HIMU–EM1–EM2 sources.

Recently, it was estimated that the HIMU end-member reservoir most likely has δ^7Li values higher than +7.4‰ from the results of Mangaia OIB (Polynesia) [18,19]. Based on Li isotopic data, Nishio et al. [18,19] proposed the HIMU component originated from the dehydrated residue of the deeper, less altered part of subducted oceanic crust. Thus, the Li isotopic data suggest a model in which the EM1 and HIMU sources may originate from different parts of a recycling oceanic crust, with the EM1 source including the upper part of the crust that is absent from the HIMU source. This is essentially the same as the models proposed previously [78–80], but with the Li isotopic data requiring uppermost, highly altered basaltic crust as well as pelagic sediment in the EM1 source, but not so in the HIMU end-member. Whereas the Pb, Sr, and Nd isotopic signatures are dominated by any contribution from sediments to the source, Li is more sensitive to the basaltic crust alteration profile and should be able to distinguish suite variations in the parts of basaltic crust that are trapped by OIBs.

6. Conclusions

In conclusion, we emphasize the following points:

- Extremely low δ^7Li values ($\delta^7Li \sim -17$‰) have been measured in CPXs in many mantle-derived ultramafic xenoliths from SW Japan (Kurose and Takashima) and FE Russia (Sveyagin, Ennokentiev, and Fevralsky). These δ^7Li values are unusually low, in comparison with the previously reported δ^7Li values of mantle-derived samples such as volcanic rocks (+1.4 to +11.2‰) [2,7,10,12–19].
- These low δ^7Li data ($\delta^7Li \sim -17$‰) are not due to analytical problems. The reasons are:
  - In a similar manner, measured δ^7Li values of fresh N-MORB glasses were found to be $+3.2 \pm 1.4$‰ (2σ, $n = 8$) [16], which is within the range of previously documented fresh MORB data (+1.5 to +6.8‰ [2,10]).
  - The samples with low δ^7Li values have high Li abundances: the FE Russia (5–11 ppm Li) and Kurose (11–24 ppm Li).
  - The Sikhote-Alin δ^7Li data correlate well with both $^{143}Nd/^{144}Nd$ and $^{87}Sr/^{86}Sr$.
  - Most typical, positive δ^7Li values were measured in mantle-derived ultramafic xenoliths from Ichino-megata and Bullenmerri (+4 to +7‰).
  - There is no difference between the Si (Mg) contents of the CPXs with extremely low δ^7Li and those with positive δ^7Li values (Table 4).
  - Repeatedly measured δ^7Li values of En2I (−17.1‰ and −16.9‰), which is the lowest δ^7Li sample, agree within analytical error (± 0.8‰, 2σ). (Two analyses were prepared from different aliquots in a xenolith.)

- Following dehydration at a subduction zone, the δ^7Li value of subducted highly altered MORB is likely to become very low relative to less altered MORB [9]. Therefore, we propose that Li of a metasomatic agent with an extremely low δ^7Li value is derived from subducted highly altered basalt, as observed in samples of the uppermost part of altered oceanic crust.
- Based on the Sr–Nd isotopic systematics and coexistent hydrous mineral, metasomatic agents of the Sikhote-Alin and Bullenmerri samples are classified into anhydrous EM1-type and hydrous EM2-type, respectively. Therefore, we infer that anhydrous EM1-like metasomatic agent has an extremely low δ^7Li value, whereas hydrous EM2-like metasomatic agent has a positive δ^7Li value.
- Li isotopic data suggest a model in which the HIMU and EM1 sources originate from different parts of a recycling oceanic crust, with the EM1 source including the upper part of the crust that is absent from the HIMU source. This is essentially the same as the models proposed previously [78–80], but with the Li isotopic data requiring uppermost, highly altered basaltic crust as well as pelagic sediment in the EM1 source, but not so in the HIMU endmember.

Acknowledgements

This manuscript benefited from thoughtful and constructive reviews and English improvement by Monica Handler and Jim Gill. We are grateful to Suzanne Y. O'Reilly for providing the Australian samples. Sincere thanks are extended to Thomas Zack for his permission to quote their results in advance of publication. Thanks are due to K. Suyehiro, W. Soh, and all DSRD (JAMSTEC) members who make every effort to produce an excellent research environment for YN. We would like to thank S. Nakada for supporting this work. Special thanks to S. Fukuda, Y. Sahoo, T. Hanyu, R. Tatsuta, S. Tokunaga, Y. Watanabe, and Y. Orihashi for maintenance of the laboratory. Comments from N. Abe, K. Sato, H. Kumagai, H. Sugioka, Y. Tatsumi, and A.B. Jeffcoate are also gratefully acknowledged. A JSPS Research Fellowship for Young Scientists to YN partly funded this study. This research was partly supported by a JSPS Postdoctoral Fellowship for Foreign Researchers in Japan and a grant-in-aid for scientific research to SN from the Ministry of Education, Culture, Sports, Science and Technology of Japan. This research was also partly supported by the Unzen Scientific Drilling Project and the Earthquake Research Institute cooperative research program of the University of Tokyo. Review by Tim Elliott helped to clarify the presentation and is greatly appreciated. ***[KF]***

Appendix. Difficulties with accurate Li isotopic analysis of peridotitic samples using TIMS

Accurate Li isotopic determination for low Li-concentration samples, such as peridotite, is difficult using TIMS techniques rather than the MC-ICP-MS technique. Chan et al. [81] reported extremely low δ^7Li values (-12.9‰ and -9.7‰) for peridotite (Z34) from Zabargad Island, Red Sea, although they revised the δ^7Li value to a positive value ($\delta^7\text{Li} \sim +5.0$‰) in a later publication [15]. Since the isotopic mass fractionation in TIMS is very sensitive to loading materials, it is essential to achieve complete Li separation from other elements [5,69]. Accordingly, it is desirable for TIMS measurements that the volume of the recovered fraction for Li is diminished as much as possible through Li purification using cation-exchange chromatography.

Contrary to this, it is necessary to collect all Li fractions to avoid incomplete Li recovery. A large Li isotopic fractionation occurs during cation-exchange chromatography [5,82]. Even if we lose only 1% of the Li, the Li isotopic composition of the collected portion could be changed significantly [5,82]. The leading Li fraction has a higher δ^7Li value (higher ^{7}Li/^{6}Li ratio) than the true value, while the tailing Li fraction has a lower δ^7Li value. Thus, if we lose the leading Li fraction, the recovered sample will give a lower value than the true value. On the other hand, if we lose the tail-

ing Li fraction, the recovered sample will give a higher δ^7Li value than the true value.

When compared to the MC-ICP-MS technique, accurate and precise Li isotopic measurements using the TIMS technique require a large amount of Li [6,8]. Because of the low Li content of peridotite (ca. 2 ppm), Li has to be separated from a large amount of sample by cation-exchange chromatography. In addition, peridotite is depleted in Si (enriched in Mg) compared with volcanic rock samples. Most Si, which is the major element in peridotite, evaporates during acid digestion using HF (e.g. $SiO_2+4HF \rightarrow SiF_4+2H_2O$). Consequently, the amount of ions introduced to the column separation tends to increase with decreasing Si content and increasing Mg content of the peridotitic sample. Here, it has to be stressed that all ions (including Li) tend to be eluted faster (elution peaks shift to earlier fraction) when the amount of ions loaded on the resin exceeds the resin's capacity. Therefore, the amount of ions introduced to the column separation tends to increase with decreasing Si content and increasing Mg content of the peridotitic sample.

Considering the above, the extremely low δ^7Li values observed by Chan's former analytical protocol [81] may have been produced as follows: As peridotite has a low Li concentration, a large amount of sample was needed for accurate Li isotopic measurements using the TIMS technique. In addition, the low-Si (high-Mg) concentration of peridotite leads to an increase in the amount of ions introduced into the column chromatography. Accordingly, the Li elution peak shifted to an earlier fraction as the amount of ions loaded on resin exceeded the resin's capacity. It is desirable for TIMS measurements that the volume of the recovered fraction for Li is as small as possible, while Li is purified using cation-exchange chromatography. In the manner of Chan's analytical protocol [81], such a narrow recovery position had been calibrated not with peridotite, but with seawater. Therefore, the Li would not have been recovered completely, since the Li elution peaks would have shifted to an earlier fraction. As a result of the loss of the leading Li fraction, the recovered sample gave a much lower δ^7Li value than the true value.

References

[1] W.F. McDonough, F.-Z. Teng, P.B. Tomascak, R.D. Ash, J.N. Grossman, R.L. Rudnick, Lithium isotopic composition of chondritic meteorites, in: Lunar and Planetary Science XXXIV, 2003, 1931 pp.
[2] T. Moriguti, E. Nakamura, Across-arc variation of Li isotopes in lavas and implications for crust/mantle recycling at subduction zones, Earth Planet. Sci. Lett. 163 (1998) 167–174.
[3] L.-H. Chan, J.M. Edmond, Variation of lithium isotope composition in the marine environment: A preliminary report, Geochim. Cosmochim. Acta 52 (1988) 1711–1717.
[4] C.-F. You, L.-H. Chan, Precise determination of lithium isotopic composition in low concentration natural samples, Geochim. Cosmochim. Acta 60 (1996) 905–915.
[5] T. Moriguti, E. Nakamura, High-yield lithium separation and the precise isotopic analysis for natural rock and aqueous samples, Chem. Geol. 145 (1998) 91–104.
[6] P.B. Tomascak, R.W. Carlson, S.B. Shirey, Accurate and precise determination of Li isotopic compositions by multi-collector sector ICP-MS, Chem. Geol. 158 (1999) 145–154.
[7] R.H. James, M.R. Palmer, The lithium isotope composition of international rock standards, Chem. Geol. 166 (2000) 319–326.
[8] Y. Nishio, S. Nakai, Accurate and precise lithium isotopic determinations of igneous rock samples using multi-collector inductively coupled plasma mass spectrometry, Anal. Chim. Acta 456 (2002) 271–281.
[9] T. Zack, P.B. Tomascak, R.L. Rudnick, C. Dalpe, W.F. McDonough, Extremely light Li in orogenic eclogites: The role of isotope fractionation during dehydration in subducted oceanic crust, Earth Planet. Sci. Lett. 208 (2003) 279–290.
[10] L.-H. Chan, J.M. Edmond, G. Thompson, K. Gillis, Lithium isotopic composition of submarine basalts: implications for lithium cycle in the oceans, Earth Planet. Sci. Lett. 108 (1992) 151–160.
[11] L.-H. Chan, J.C. Alt, D.A.H. Teagle, Lithium and lithium isotope profiles through the upper oceanic crust: a study of seawater-basalt exchange at ODP Sites 504B and 896A, Earth Planet. Sci. Lett. 201 (2002) 187–201.
[12] P.B. Tomascak, F. Tera, R.T. Helz, R.J. Walker, The absence of lithium isotope fractionation during basalt differentiation: new measurements by multicollector sector ICP-MS, Geochim. Cosmochim. Acta 63 (1999) 907–910.
[13] P.B. Tomascak, J.G. Ryan, M.J. Defant, Lithium isotope evidence for light element decoupling in the Panama subarc mantle, Geology 28 (2000) 507–510.
[14] P.B. Tomascak, E. Widom, L.D. Benton, S.L. Goldstein, J.G. Ryan, The control of lithium budgets in island arcs, Earth Planet. Sci. Lett. 196 (2002) 227–238.
[15] L.H. Chan, W.P. Leeman, C.-F. You, Lithium isotopic composition of Central American volcanic arc lavas: implications for modification of subarc mantle by slab-derived fluids: correction, Chem. Geol. 182 (2002) 293–300.

[16] Y. Nishio, S. Nakai, K. Hirose, T. Ishii, Y. Sano, Li isotopic systematics of volcanic rocks in marginal basins (abstr.), Geochim. Cosmochim. Acta 66 (2002) A556.
[17] L.-H. Chan, F.A. Frey, Lithium isotope geochemistry of the Hawaiian plume: Results from the Hawaii Scientific Drilling Project and Koolau Volcano, Geochem. Geophys. Geosyst. 4 (2003) 10.1029/2002GC000365.
[18] Y. Nishio, S. Nakai, T. Kogiso, H.G. Barsczus, Lithium isotopic composition of HIMU oceanic island basalts: implications for the origin of HIMU component, in: XXIII General Assembly of the International Union of Geodesy and Geophysics (IUGG 2003), 2003, 178 pp.
[19] Y. Nishio, S. Nakai, T. Kogiso, H.G. Barsczus, Lithium isotopic composition of HIMU oceanic island basalts in the Polynesian region: implications for the origin of HIMU component, submitted to Geochim. Cosmochim. Acta.
[20] D.A. Ionov, V.S. Prikhod'ko, S.Y. O'Reilly, Peridotite xenoliths in alkali basalts from the Sikhote-Alin, southeastern Siberia, Russia: trace-element signatures of mantle beneath a convergent continental margin, Chem. Geol. 120 (1995) 275–294.
[21] S. Arai, H. Hirai, K. Uto, Mantle peridotite xenoliths from the Southwest Japan arc and a model for the sub-arc upper mantle structure and composition of the Western Pacific rim, J. Mineral. Petrol. Sci. 95 (2000) 9–23.
[22] E. Takahashi, Genesis of calc-alkali andesite magma in a hydrous mantle-crust boundary: Petrology of lherzolite xenoliths from the Ichinomegata crater, Oga peninsula, northeast Japan, part II, J. Volcanol. Geotherm. Res. 29 (1986) 355–395.
[23] N. Abe, S. Arai, H. Yurimoto, Geochemical characteristics of the uppermost mantle beneath the Japan island arcs: implications for upper mantle evolution, Phys. Earth Planet. Inter. 107 (1998) 233–248.
[24] S.Y. O'Reilly, W.L. Griffin, Mantle metasomatism beneath western Victoria, Australia: I. Metasomatic processes in Cr-diopside lherzolite, Geochim. Cosmochim. Acta 52 (1988) 433–447.
[25] N. Abe, S. Arai, Y. Saeki, Hydration processes in the arc mantle: petrology of the Megata peridotite xenoliths, the Northeast Japan arc (in Japanese with English abstract), J. Mineral. Petrol. Econ. Geol. 87 (1992) 305–317.
[26] N. Abe, S. Arai, Petrographical chracteristics of ultramafic xenoliths from Megata volcano, the Northeast Japan arc, Sci. Rep. Kanazawa Univ. 38 (1993) 1–24.
[27] E. Nakamura, I. McDougall, I.H. Cambell, K-Ar ages of basalts from Higashi-Matsuura district, northwestern Kyushu, Japan and regional geochronology of the Cenozoic alkaline volcanic rocks in eastern Asia, Geochem. J. 20 (1986) 91–99.
[28] K. Uto, H. Hirai, S. Arai, K-Ar ages for Quaternary alkali basalts from Kurose, Fukuoka prefecture and Kifune, Yamaguchi prefecture, southwest Japan (in Japanese with English abstract), Bull. Geol. Surv. Jpn. 44 (1993) 693–698.
[29] E. Takahashi, Petrologic model for the crust and upper mantle of the Japanese island arcs, Bull. Volcanol. 41 (1978) 529–547.
[30] I.A. Nicholls, E.B. Joyce, Newer volcanics, in: R.W. Johnson (Ed.), Intraplate Volcanism in Eastern Australia and New Zealand, Cambridge Univ. Press, 1989, 408 pp.
[31] Y. Tatsumi, K. Sato, T. Sano, R. Arai, V.S. Prikhodko, Transition from arc to intraplate magmatism associated with backarc rifting: evolution of the Sikhote Alin volcanism, Geophys. Res. Lett. 27 (2000) 1587–1590.
[32] Y. Tatsumi, High magnesian andesites in the Setouchi volcanic belt, southwest Japan and their possible relation to the evolutionary history of the Shikoku inter-arc basin, in: S. Uyeda, T. Hilde (Eds.), Geodynamics of the Western Pacific-Indonesian Region, Geodynam. Ser. 11, AGU, Washington, DC, 1983, pp. 331–341.
[33] Y. Tatsumi, Migration of fluid phases and genesis of basalt magmas in subduction zones, J. Geophys. Res. 94 (1989) 4697–4707.
[34] E. Nakamura, I.H. Cambell, S. Sun, The influence of subduction process on the geochemistry of Japanese alkaline basalts, Nature 316 (1985) 55–58.
[35] E. Nakamura, I.H. Campbell, M.T. McCulloch, S.-S. Sun, Chemical geodynamics in a back-arc region around the Sea of Japan: Implications for the genesis of alkaline basalts in Japan, Kurose and China, J. Geophys. Res. 94 (1989) 4634–4654.
[36] H. Iwamori, Zonal structure of Cenozoic basalts related to mantle upwelling in Southwest Japan, J. Geophys. Res. 96 (1991) 6157–6170.
[37] H. Iwamori, Degree of melting and source composition of Cenozoic basalts in southwest Japan: evidence for mantle upwelling by flux melting, J. Geophys. Res. 97 (1992) 10983–10995.
[38] M. Faure, B. Natal'in, The geodynamic evolution of the eastern Eurasian margin in Mesozoic times, Tectonophysics 208 (1992) 397–411.
[39] A. Miyashiro, Hot regions and the origin of marginal basins in the western pacific, Tectonophysics 122 (1986) 195–216.
[40] Y. Song, F.A. Frey, X. Zhi, Isotopic systematics of Hannuoba basalts, eastern China: implications for their petrogenesis and the composition of subcontinental mantle, Chem. Geol. 85 (1990) 35–52.
[41] S. Okamura, R.J. Arculus, Y.A. Martynov, H. Kagami, T. Yoshida, Y. Kawano, Multiple magma sources involved in marginal-sea formation; Pb, Sr, and Nd isotopic evidence from the Japan Sea region, Geology 26 (1998) 619–622.
[42] S. Okamura, Y.A. Martynov, K. Furuyama, K. Nagao, K-Ar ages of the basaltic rocks from Far East Russia: Constraints on the tectono-magmatism associated with the Japan Sea opening, Island Arc 7 (1998) 271–282.
[43] H. Sumino, S. Nakai, K. Nagao, K. Notsu, High $^{3}He/^{4}He$ ratio in xenoliths from Takashima: evidence for plume type volcanism in southwestern Japan, Geophys. Res. Lett. 27 (2000) 1211–1214.

[44] T. Matsumoto, M. Honda, I. McDougall, I. Yatsevich, S.Y. O'Reilly, Plume-like neon in a metasomatic apatite from the Australian lithospheric mantle, Nature 388 (1997) 162–164.
[45] W.L. Griffin, S.Y. Wass, J.D. Hollis, Ultramafic xenoliths from Bullenmerri and Gnotuk maars, Victoria, Australia: petrology of a subcontinental crust-mantle transition, J. Petrol. 25 (1984) 53–87.
[46] E. Takahashi, Thermal history of lherzolite xenoliths. 1. Petrology of lherzolite xenoliths from the Ichinomegata Crater, Oga Peninsula, northeast Japan, Geochim. Cosmochim. Acta 44 (1980) 1643–1658.
[47] N. Abe, S. Arai, H. Yurimoto, Texture-dependent geochemical variations of sub-arc mantle peridotite from Japan island arcs, in: Proc. 7th Int. Kimberlite Conf., 1998, pp. 13–22.
[48] N. Imai, S. Terashima, S. Itoh, A. Ando, 1994 compilation values for GSJ reference samples, 'Igneous rock series', Geochem. J. 29 (1995) 91–95.
[49] H. Kurasawa, Strontium isotope composition of the volcanic rocks from Fuji, Hakone and Izu area, Rep. Geol. Surv. Jpn. 35 (1984) 637–659.
[50] A. Ando, K. Shibata, Isotope data and rare gas compositions of GSJ rock reference samples, 'Igneous rock series', Geochem. J. 22 (1988) 149–156.
[51] H. Kagami, H. Yokose, H. Honma, $^{87}Sr/^{86}Sr$ and $^{143}Nd/^{144}Nd$ ratios of GSJ rock reference samples; JB-1a, JA-1 and JG-1a, Geochem. J. 23 (1989) 209–214.
[52] O. Okano, R. Kanazawa, H. Tosa, H. Matsumoto, Sr, Nd and Ce isotopic measurements of GSJ standard rocks using MAT 262 equipped with variable multi-collector system, in: Annu. Meet., Geochem. Soc. Jpn., 1989, 268 pp. (in Japanese).
[53] K. Notsu, Y. Hirao, Rapid and precise measurement of strontium isotope ratio using an automatic mass spectrometer, Hozon-Kagaku 29 (1990) 51–58.
[54] Y. Arakawa, $^{143}Nd/^{144}Nd$ ratio of twelve GSJ rock reference samples and reproducibility of the data, Geochem. J. 26 (1992) 105–109.
[55] S. Iizumi, K. Maehara, P.A. Morris, Y. Sawada, Sr isotope data of GSJ rock reference samples, Mem. Fac. Sci. Shimane Univ. 28 (1994) 83–86.
[56] C.-k. Na, T. Nakano, K. Tazawa, M. Sakagawa, T. Ito, A systematic and practical method of liquid chromatography for the determination of Sr and Nd isotopic ratios and REE concentrations in geological samples, Chem. Geol. 123 (1995) 225–237.
[57] Y. Orihashi, J. Maeda, R. Tanaka, R. Zeniya, K. Niida, Sr and Nd isotopic data for the seven GSJ rock reference samples; JA-1, JB-1a, JB-2, JB-3, JG-1a, JGb-1 and JR-1, Geochem. J. 32 (1998) 205–211.
[58] D.R. Porcelli, R.K. O'Nions, S.J.G. Galer, A.S. Cohen, D.P. Mattey, Isotopic relationships of volatile and lithophile trace elements in continental ultramafic xenoliths, Contrib. Mineral. Petrol. 110 (1992) 528–538.
[59] J. Yamamoto, Investigation of the subcontinental mantle based on noble gas isotopes, petrological and spectroscopic studies of Siberian mantle xenoliths, Doctor Thesis, Univ. of Tokyo, 2001.
[60] W.L. Griffin, S.Y. O'Reilly, A. Stabel, Mantle metasomatism beneath western Victoria, Australia: II. Isotopic geochemistry of Cr-diopside lherzolites and Al-augite pyroxenites, Geochim. Cosmochim. Acta 52 (1988) 449–459.
[61] A. Zindler, S. Hart, Chemical geodynamics, Annu. Rev. Earth Planet. Sci. 14 (1986) 493–571.
[62] M.A. Menzies, S.Y. Wass, CO_2- and LREE-rich mantle below eastern Australia: a REE and isotopic study of alkaline magmas and apatite-rich mantle xenoliths from the Southern Highlands Province, Australia, Earth Planet. Sci. Lett. 65 (1983) 287–302.
[63] M. Tatsumoto, Y. Nakamura, DUPAL anomaly in the Sea of Japan: Pb, Nd, and Sr isotopic variations at the eastern Eurasian continental margin, Geochim. Cosmochim. Acta 55 (1991) 3697–3708.
[64] A.R. Basu, W. Junwen, H. Wankang, X. Guanghong, M. Tatsumoto, Major element, REE, and Pb, Nd and Sr isotopic geochemistry of Cenozoic volcanic rocks of eastern China: implications for their origin from suboceanic-type mantle reservoirs, Earth Planet. Sci. Lett. 105 (1991) 149–169.
[65] M. Tatsumoto, A.R. Basu, H. Wankang, W. Junwen, X. Guanghong, Sr, Nd, and Pb isotopes of ultramafic xenoliths in volcanic rocks of Eastern China: enriched components EMI and EMII in subcontinental lithosphere, Earth Planet. Sci. Lett. 113 (1992) 107–128.
[66] M. Zhang, P. Suddaby, R.N. Thompson, M.F. Thirlwall, M.A. Menzies, Potassic volcanic rocks in NE China: geochemical constraints on mantle source and magma genesis, J. Petrol. 36 (1995) 1275–1303.
[67] L. Zhang, L.-H. Chan, J.M. Gieskes, Lithium isotope geochemistry of pore waters from ocean drilling program Sites 918 and 919, Irminger Basin, Geochim. Cosmochim. Acta 62 (1998) 2437–2450.
[68] M. Zhang, P. Suddaby, S.Y. O'Reilly, M. Norman, J. Qiu, Nature of the lithospheric mantle beneath the eastern part of the Central Asian fold belt: mantle xenolith evidence, Tectonophysics 328 (2000) 131–156.
[69] J. Hoefs, M. Sywall, Lithium isotope composition of Quaternary and Tertiary biogene carbonates and a global lithium isotope balance, Geochim. Cosmochim. Acta 61 (1997) 2679–2690.
[70] Y. Huh, L.-H. Chan, L. Zhang, J.M. Edmond, Lithium and its isotopes in major world rivers: implications for weathering and the oceanic budget, Geochim. Cosmochim. Acta 62 (1998) 2039–2051.
[71] L.-H. Chan, M. Kastner, Lithium isotopic compositions of pore fluids and sediments in the Costa Rica subduction zone: implications for fluid processes and sediment contribution to the arc volcanoes, Earth Planet. Sci. Lett. 183 (2000) 275–290.
[72] T. Zack, S.F. Foley, T. Rivers, Equilibrium and disequilibrium trace element partitioning in hydrous eclogites (Trescolmen, Central Alps), J. Petrol. 43 (2002) 1947–1974.

[73] L.D. Benton, I. Savoy, J.G. Ryan, Recycling of subducted lithium in forearcs: Insights from a serpentine seamount, EOS Trans. AGU 80 (1999) S349.
[74] K. Kobayashi, R. Tanaka, T. Moriguti, K. Shimizu, E. Nakamura, Lithium, boron, and lead isotope systematics on glass inclusions in olivine phenocrysts from Hawaiian lavas (abstr.), Geochim. Cosmochim. Acta 67 (2003) A223.
[75] M.F. Roden, T. Trull, S.R. Hart, F.A. Frey, New He, Nd, Pb, and Sr isotopic constraints on the constitution of the Hawaiian plume: Results from Koolau Volcano, Oahu, Hawaii, USA, Geochim. Cosmochim. Acta 58 (1994) 1431–1440.
[76] R. Tanaka, E. Nakamura, E. Takahashi, Geochemical evolution of Koolau Volcano, Hawaii, in: E. Takahashi, P.W. Lipman, M.O. Garcia, J. Naka, S. Aramaki (Eds.), Hawaiian Volcanoes: Deep Underwater Perspective, AGU Geophys. Monogr. 128, American Geophysical Union, Washington, DC, 2002, pp. 311–332.
[77] S.R. Hart, D.C. Gerlach, W.M. White, A possible new Sr-Nd-Pb mantle array and consequences for mantle mixing, Geochim. Cosmochim. Acta 50 (1986) 1551–1557.
[78] B.L. Weaver, The origin of ocean island basalt end-member compositions: Trace element and isotopic constraints, Earth Planet. Sci. Lett. 104 (1991) 381–397.
[79] C. Chauvel, A.W. Hofmann, P. Vidal, HIMU-EM: The French Polynesian connection, Earth Planet. Sci. Lett. 110 (1992) 99–119.
[80] M. Roy-Barman, C.J. Allègre, $^{187}Os/^{186}Os$ in oceanic island basalts: tracing oceanic crust recycling in the mantle, Earth Planet. Sci. Lett. 129 (1995) 145–161.
[81] L.-H. Chan, W.P. Leeman, C.-F. You, Lithium isotopic composition of Central American Volcanic Arc lavas: implications for modification of subarc mantle by slab-derived fluids, Chem. Geol. 160 (1999) 255–280.
[82] T.I. Taylor, H.C. Urey, Fractionation of the lithium and potassium isotopes by chemical exchange with zeolites, J. Chem. Phys. 6 (1938) 429–438.